


 Cite this: *RSC Adv.*, 2021, **11**, 23010

# Improved mechanical performances of unidirectional jute fibre composites developed with new fibre architectures

 Mahmudul Hasan,<sup>a</sup> Abu Saifullah,<sup>b</sup> Hom N. Dhakal,<sup>b</sup> \*<sup>b</sup> Shahjalal Khandaker<sup>a</sup> and Forkan Sarker \*<sup>a</sup>

This study presents the mechanical performance enhancements of jute fibre composites, manufactured from two newly developed novel jute fibre unidirectional (UD) preforms, namely, stitching-based and sizing-based examples. To increase the use of jute fibres, which are naturally abundant and inexpensive, and to provide research into the use of mechanically advantageous continuous unidirectional (UD) preforms in composites (which are still limited in use), this study employed polyvinyl alcohol (PVA) sizing and stitching techniques, thus increasing the abilities of jute fibres to withstand higher loads and enabling them to be used for lightweight structural applications. Alkali treatment was used on jute fibres in stitched and sized preforms, and bamboo slices were introduced to the jute preforms to further optimize the mechanical properties. The jute composites exhibited significant mechanical property enhancements, with maximum improvement observed in the case of the PVA-sized alkali-treated specimen, thanks to the excellent compatibility between the sized and alkali-treated jute fibres.

 Received 5th May 2021  
 Accepted 17th June 2021

DOI: 10.1039/d1ra03515k

[rsc.li/rsc-advances](http://rsc.li/rsc-advances)

## 1. Introduction

Jute fibre, one of the longest natural fibres (*i.e.*, longer than flax, sisal, hemp, kapok, ramie, *etc.*), is largely grown in Bangladesh, India, and China. Jute fibre can be used as a replacement for synthetic fibres, such as glass fibres, in many structural composite applications where stiffness is a primary requirement. In addition, the environmental hazards of glass-fibre-based composite production are becoming a major issue related to composite manufacturing, as highlighted by environmental groups around the world.<sup>1</sup> As a promising bio-based material, jute fibre offers many benefits over glass fibres, specifically a low specific weight, excellent thermal and acoustic insulation abilities, biodegradability, and low production costs, which ultimately have made this fibre a priority for composite manufacturers.<sup>2</sup> However, to date, limited research has been reported in the literature aimed at promoting the use of jute fibre for high mechanical performance composite applications.

One of the major concerns surrounding the use of jute and other natural fibres for composite applications is related to their lack of reinforcing abilities due to the poor tensile properties of dry fibre architectures.<sup>3</sup> For example, woven, randomly oriented non-woven, and knitted structures generally involve

yarn twisting, fabric crimping, and shorter fibre lengths in non-woven fabrics, adversely affecting the mechanical properties of jute fibre composites.<sup>4,5</sup> Previous studies<sup>2,5,6</sup> have also suggested that the best mechanical properties can only be achieved in a composite if all the fibres are printed in a parallel direction inside the composite. In order to optimize the mechanical properties of natural fibre reinforced composites, it is recommended that the natural fibres should be aligned in a parallel or unidirectional (UD) arrangement, similar to how glass and carbon fibres are normally arranged in structural composites.

Another major problem related to natural fibres such as jute is the incompatibility between the hydrophilic natural fibre and the hydrophobic polymer matrices used in composites, leading to lower mechanical properties and poorer long-term durability being shown by jute fibre composites. Impurities such as lignin, hemicellulose, and other non-cellulose materials are responsible for this problem.<sup>5,7</sup> Various physical and chemical processes have been reviewed by many researchers<sup>2,8,9</sup> for removing impurities from jute fibres. Alkali treatment, which is also commonly known as mercerization, is mainly used for the modification of jute fibres.<sup>10,11</sup> Previous studies have suggested that the prolonged exposure of jute fibres to low-concentration alkali solution is an effective way to retain the structural integrity of jute fibre while increasing the compatibility at the fibre/matrix interface in composites.<sup>5,8</sup>

In order to enhance the mechanical properties of jute composites, a combination of improved fibre wettability and defined fibre alignment was employed in the present study, where new dry UD jute fibre architecture based preforms with

<sup>a</sup>Dept. of Textile Engineering, Dhaka University of Engineering & Technology, Gazipur, 1700, Bangladesh. E-mail: [forkan@duet.ac.bd](mailto:forkan@duet.ac.bd)

<sup>b</sup>Advanced Polymers and Composites (APC) Research Group, School of Mechanical and Design Engineering, University of Portsmouth, Portsmouth PO1 3DJ, UK. E-mail: [hom.dhakal@port.ac.uk](mailto:hom.dhakal@port.ac.uk)



and without alkali treatment were developed. To manufacture the UD jute fibre preforms, two novel approaches were used separately – the stitching and sizing of jute fibres were compared with each other to understand their effects on the mechanical properties of UD jute fibre composites. It was reported in a previous study that the sizing of fibres can affect the interfacial properties, such as the fibre packing and drapability, of composites because of the holding down of individual fibres together, maintaining fibre–fibre cohesion/autohesion.<sup>1</sup> It has been recommended that the use of only 1% of epoxy-compatible sizing mist is enough to hold fibres together to form a UD preform with pressing. On the other hand, the stitching of UD jute preforms is considered to be an effective way to remove any alterations in fibre direction during draping operations before composite manufacturing, since, recently, various studies have suggested that stitch formation on preforms using an industrial sewing machine can hold fibres in the same direction and strongly influence the interfacial, interlaminar, and anti-damage properties of natural fibre composites.<sup>12–15</sup>

Composite hybridization is a very effective approach that is particularly suitable for improving the mechanical properties of natural fibre composites in a cost-effective way, allowing them to replace the use of expensive and non-degradable glass or carbon fibre composites for various applications.<sup>16–19</sup> Bamboo fibre, known as ‘natural glass fibre’ with a tensile strength of 610 MPa, has attracted the interests of researchers as it takes the form of naturally occurring unidirectional long parallel cellulose fibres.<sup>20</sup> Bamboo fibre offers a high specific strength, carbon sequestration abilities, recycling potential, and rapid growth compared with wood, and it is suitable for various applications.<sup>21</sup> The bamboo plant commercially known as ‘Mulli Bash’ in Bangladesh (scientific name: *Bambusa polymorpha*) can be easily peeled into slices to make products with the desired shapes. Bamboo slices were hybridized with both newly developed stitched and sized UD jute fibre preforms in this study to check the compatibility of bamboo slices with the stitched and sized UD jute preforms and, also, to further enhance the mechanical properties of the jute composites in a cheaper way.

In light of the above discussion, the aim of this research was to develop novel stitching- and sizing-based highly packed UD jute fibre preforms separately and to also hybridize them with bamboo slices in order to manufacture high mechanical performance and cost-effective jute fibre composites to replace

the current trend of using synthetic glass fibres for structural composites applications. According to the best knowledge of the authors, novel stitching- and sizing-based UD preforms were developed for the first time in this work. Both stitched and sized UD jute preforms were developed with alkali-treated and untreated jute fibres to modify and analyze the interfacial properties between the fibres and matrix. Fibre characterization was carried out using optical microscopy and scanning electron microscopy (SEM). Chemical and thermal analysis of fibres (alkali and sizing treatment) was conducted using FTIR and TGA, respectively. The mechanical properties of the developed composites were evaluated *via* tensile and flexural testing. The compatibility of bamboo slices with the hybridized stitched and sized jute fibre preforms was assessed in terms of the mechanical and thermo-mechanical properties of the composites. The dynamic mechanical properties were evaluated using a dynamic mechanical thermal analysis (DMTA) instrument in order to understand the storage and damping behavior of the UD jute fibre and hybrid (jute/bamboo) composites. It is believed that the developed novel UD preforms and bamboo hybridization shown in this work will be helpful for enhancing the use of jute composites for higher-load-bearing applications.

## 2. Experimental method

### 2.1. Materials

Commercially available jute slivers for jute yarn manufacturing (2nd drawing machine output) were collected from UMC Jute Mills, Narsingdi, Bangladesh. These experimental slivers consisted of 80% Bangle Tossa-C (B.T.C) and 20% Bangle White-C (B.W.C) jute fibres, and the sliver weight and length were ~1.8 kg and ~91 m, respectively. The jute fibre diameter, density, tensile strength, and modulus were ~40  $\mu\text{m}$ , ~1.38  $\text{g cm}^{-3}$ , ~280 MPa, and ~29 GPa, respectively, according to the supplier information. The collected jute sliver had an average thickness of 0.55 ( $\pm 0.09$ ) mm, measured based on the ASTM D5729-97 standard and an area density of 290 ( $\pm 58$ ) GSM (grams per square metre) (see the untreated preform information in Table 1). Bamboo slices with a thickness of ~0.8 mm were extracted mechanically from bamboo (*Bambusa polymorpha*) plants, which are abundantly available near Dhaka City, Bangladesh. Unmodified liquid epoxy (Lapox B-11, 5.25 Eq/kg) and aliphatic polyamine hardener (Lapox K6) were collected from Atul Ltd, Gujarat, India. GP 5501 NF, a synthetic coarse dispersion of polyvinyl acetate homopolymer, was collected from Aristek

Table 1 The physical properties of the developed preforms made of jute fibres and bamboo

Preform type	ID	Preform width (mm)	Preform thickness (mm)	Preform area density (GSM)
Untreated (no treatment at all)	UT	120	0.55 $\pm$ 0.09	290 $\pm$ 58
Stitched, alkali-untreated	SUT	120	0.55 $\pm$ 0.11	310 $\pm$ 45
Stitched, alkali-treated	ST		0.58 $\pm$ 0.13	315 $\pm$ 58
Sized, alkali-untreated	BUT	120	0.60 $\pm$ 0.08	320 $\pm$ 43
Sized, alkali-treated	BT		0.62 $\pm$ 0.09	325 $\pm$ 44
Bamboo slice	BB	100	0.8 $\pm$ 0.02	380 $\pm$ 10



High Polymer, West Java, Indonesia. Double-ply 100% polyester stitching thread with a linear density of 40 tex, a ticket no. of 75, a breaking force of 52 N, and elongation of 3–5% was collected from Coats Dhaka, Bangladesh, to stitch the fibres.

## 2.2. Fibre surface treatment (alkali and sizing treatments)

Based on previously reported processes, unidirectional jute slivers were alkali-treated very carefully in 0.5% NaOH solution at a fibre to liquid ratio of 1 : 30 (w/w) for 24 h, keeping the fibre alignment unchanged.<sup>5</sup> These alkali treatment conditions were selected to remove hemicellulose, *etc.*, and to improve the fibrillar packing of fibres without any fibre quality degradation. After alkali treatment, the treated slivers were dried at 80 °C for 5 h. The sizing treatment of jute fibres is explained below with sizing-based preform details. Here, for the chemical characterization and analysis of fibres, a coding system was used; the untreated jute fibres are referred to as UT, alkali-treated jute fibres are referred to as AT, sizing (or binder) treatment samples using untreated and alkali-treated fibres are referred to as BUT and BT, respectively, and bamboo fibres are referred to as BB.

## 2.3. Fibre and preform characterization

A scanning electron microscope (SEM) (Philip XL-30) was used to conduct microscopic observations of jute fibres both with and without various alkali and sizing treatments. Chemical

analysis of untreated and treated jute fibres was performed with the help of Fourier-transform infrared (FTIR) spectroscopy. The thermal properties of fibres with/without treatment were investigated using a TA instrument (TA Q50, UK) within the temperature range of 25 to 600 °C at a heating rate of 10 °C min<sup>-1</sup> under a nitrogen atmosphere.

The ASTM D5729-97 standard method was followed to measure the average thicknesses of dry fibre preforms. The area densities of the preforms were calculated in units of grams per square meter (GSM) *via* taking the weights of samples with a size of 100 mm × 50 mm. At least five specimens were considered when measurements were taken. Cross-sectional images of the composites were obtained using an optical microscope (Keyence digital microscope VHX-500F, UK).

## 3. Methodology

### 3.1. The development of unidirectional preforms

**Stitching-based preform.** Stitching-based unidirectional jute fibre preforms were developed using a simple industrial lock stitch sewing machine (Juki DDL-9000B). The unidirectional jute sliver (see Fig. 1a) was placed transversely into the feeding zone of the sewing machine. The stitching operation was carried out in the stitching zone under the sewing needle to produce Lockstitch-301-type stitches with a stitch density of 9 SPI in the transverse direction of the sliver, keeping a minimum

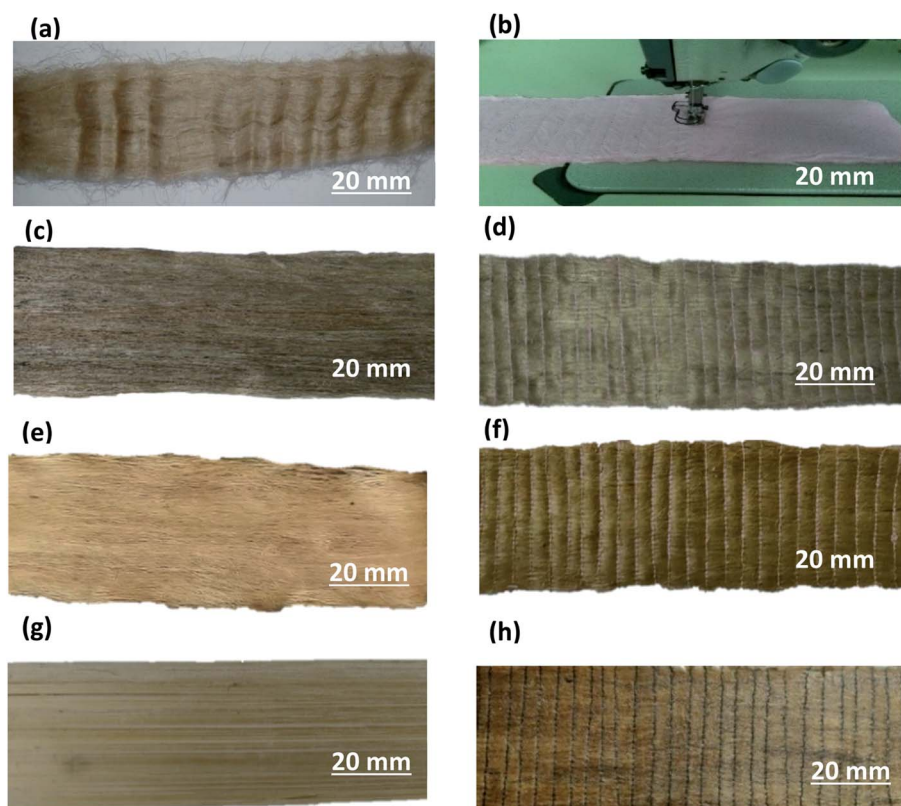


Fig. 1 The jute fibre UD preforms and composites developed in this study: (a) a drawn sliver collected from a supplier, (b) the stitching operation on a jute sliver, (c) a sized alkali-untreated jute fibre preform, (d) a stitched alkali-untreated preform, (e) a sized alkali-treated preform, (f) a stitched alkali-treated preform, (g) a bamboo preform, and (h) a stitched alkali-treated jute fibre preform composite.



distance of 10 mm between the stitch lines (see Fig. 1b). A 10 mm stitch line distance was found to be good enough to create stitch lines smoothly without any fibre crimping (see Fig. 1d). After the stitching operation, the stitched jute fibre preform was treated in alkali solution, as discussed above (see Fig. 1f).

**Sizing-based preform.** Sized unidirectional preforms were also developed with and without treating the jute fibres in alkali solution (see Fig. 1c and e). For the sizing treatment, alkali-treated and untreated jute fibres were dipped into polyvinyl alcohol (PVA) (1%) sizing solution with a material to water ratio of 1 : 10 (w/w) for 30 min to bind the individual fibres. After the sizing process, the fibres were passed through a squeezing roller to remove excess sizing material from the surfaces of the jute fibres, and they were subsequently oven-dried at 80 °C in order to complete the binding of the sizing material on the jute fibres.

**Bamboo-slice extraction process.** Locally collected 8 m long cylindrically shaped bamboo stems or culms were cut through the center of the cylindrical culm along its length with the help of a saw to obtain culms with a half-cylindrical shape. The nodes were removed with a knife from the cutaway bamboo culms. Then the body of the cutaway culm was taken off and split into slices along its length, taking special care to maintain uniform slice thicknesses and widths. The dimensions of the bamboo slices were measured to be as follows: length, 400 mm; width, 120 mm; and average thickness, ~0.8 mm. The extracted bamboo slices were dried in the sun for 5 days, followed by oven

exposure at a temperature of 80 °C for 8 h to complete moisture removal. The preforms made from bamboo slices were coded as BB (see Fig. 1g).

### 3.2. Composite fabrication

Unidirectional jute composite laminates comprising stitched and sized preforms were fabricated using a compression moulding technique. A room-temperature curing epoxy resin mixture was prepared with a resin to hardener ratio of 100 : 10, and this was applied onto the dried jute fibre preforms using a wet lay-up method, maintaining a constant known fibre-to-resin weight ratio. A total of eight dry fibre preform layers were used for making unidirectional composites in the wet lay-up process with a minimum composite thickness of 3 mm (see Fig. 1h and 2). Finally, the impregnated preforms were compacted at a pressure of approximately 14 MPa in order to get the high-fibre-volume composites recommended by a previous study,<sup>1</sup> realizing that the fibre mechanical properties are not affected by this pressure. Samples were left under compression for 24 h in order to obtain composites with uniform thickness. The applied pressure and curing time remained constant to obtain composite homogeneity. In the case of hybrid composites, bamboo slices were also impregnated using the wet lay-up method and interleaved with stitching- and sizing-based preforms, using similar pressure and curing time conditions to the other composites in this work.

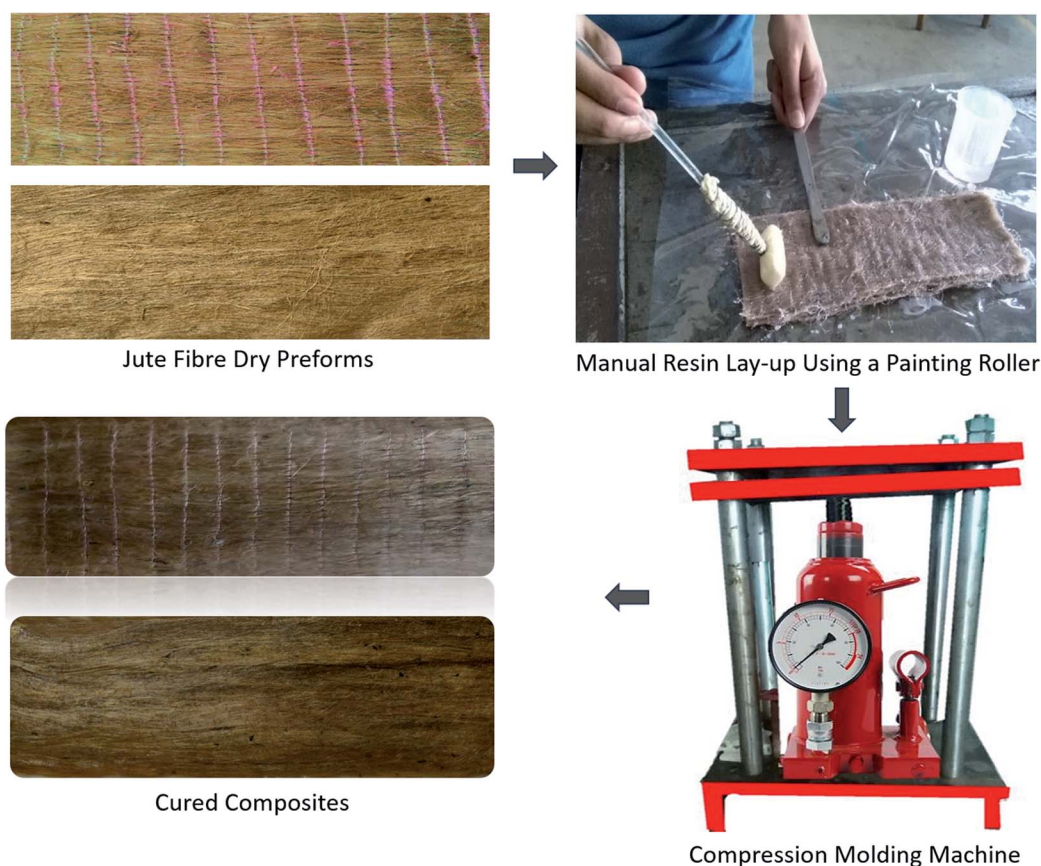


Fig. 2 Photographs of the composite fabrication process.



All the produced composites were coded in this paper based on the preform manufacturing process used. A list of the codes is given as follows: the untreated fibre preform (without any treatment) is referred to as UT; the stitched alkali-untreated preform composite is referred to as SUT; the stitched alkali-treated preform composite is referred to as ST; the PVA-sized alkali-untreated preform composite is referred to as BUT; the PVA-sized alkali-treated preform composite is referred to as BT; the stitched alkali-untreated and -treated preforms with an additional bamboo slice are referred to as SUTB and STB, respectively; and the PVA-sized alkali-untreated and -treated preforms with an additional bamboo slice are referred to as BUTB and BTB, respectively. The use of two bamboo slices alone reinforced with epoxy is coded here as BB.

### 3.3. Composite density and fibre volume fraction measurements

Fibre and composite densities were measured based on the ASTM-D3800-99 standard method using an AJ5OL (Mettler Toledo, UK) analytical balance. The water immersion method has been used extensively for measuring the densities of natural fibres and their hybrid composites.<sup>1,22–24</sup> Cut sample edges were coated with epoxy resin so that water did not penetrate into the composites. According to this method, the samples were weighed in air and then separately under immersed conditions in water. Eqn (1) was applied in order to obtain the experimental densities of the composites:

$$\rho_{\text{composite}} = W_{\text{dry}} / (W_{\text{dry}} - W_{\text{wet}}) \quad (1)$$

After determining the densities of the composites, fibre volume fractions of the composites were determined *via* taking the known weight of dry fibres and composites and calculating the resin weight. Knowing all the weights of the materials, the fibre volume fractions could be calculated using the following eqn (2):

$$V_{\text{fibre}} = \frac{\rho_{\text{composite}}}{\rho_{\text{fibre}}} \times W_{\text{fibre}} \quad (2)$$

### 3.4. Mechanical testing of composites

Tensile tests were performed in accordance with the ASTM D3039 standard method using an AG-X plus universal testing machine (Japan) equipped with a properly calibrated 100 kN load cell. The load cell was selected based on a projection of the maximum breaking load of the composite materials tested in the laboratory. Test specimens with a length of 250 mm and width of 15 mm were prepared for tensile testing according to the test standards. Five specimens from each composite type were tested. The speed of the machine was kept constant at 2 mm min<sup>-1</sup> during testing. Tensile modulus values of the composites were calculated from the slope of the stress-strain curve in the strain range of 0.1–0.3%. The mean values of the tested specimens of each sample type were calculated after testing. Three-point bending testing was performed on an AG-X plus universal testing machine (Japan) based on the ASTM-D790 standard method to characterize the flexural properties of the composites. Samples with a length of 127 mm and a width of

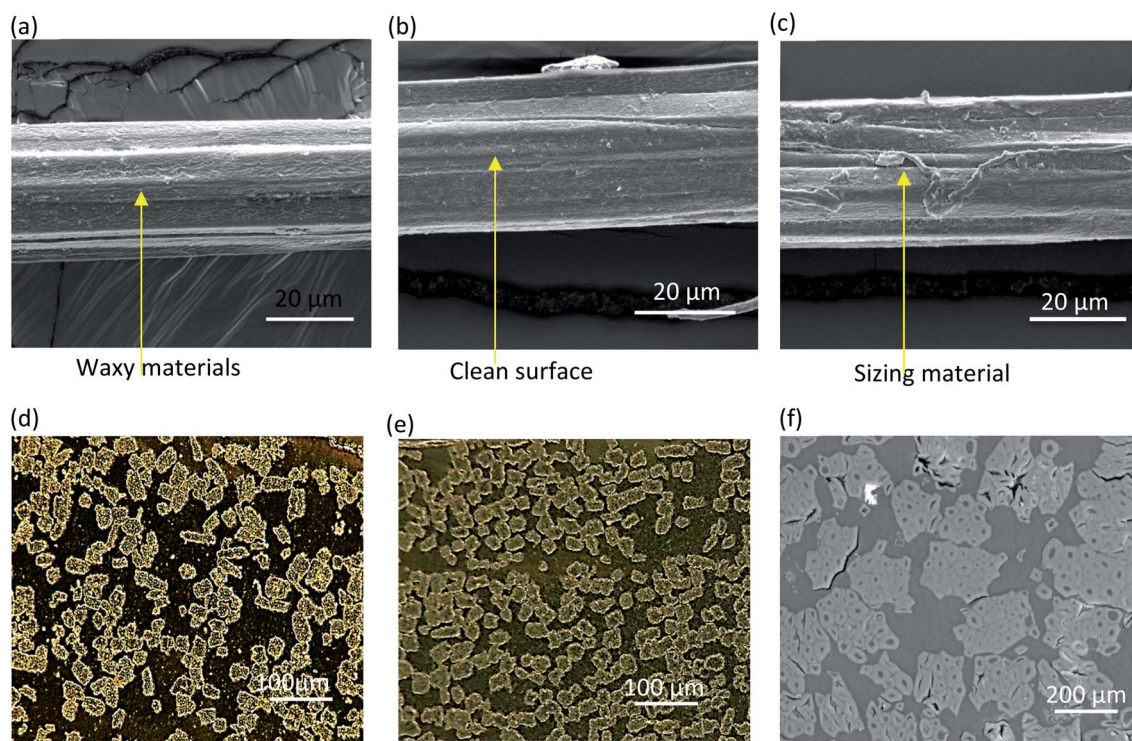


Fig. 3 Scanning electron microscopy images of jute fibres: (a) an UT (untreated) fibre, (b) an AT (alkali-treated) fibre, and (c) a BT (sized alkali-treated) fibre. Cross-sectional images of the composites under an optical microscope: (d) the UT (untreated) composite and (e) the BT (sized alkali treated) composite. (f) An SEM microscale cross-sectional image of the UT composite.



12.4 mm with a support span of 96.3 mm were used in these tests. The machine was loaded with a properly calibrated 10 kN load cell with a constant crosshead speed of 1 mm min<sup>-1</sup>, according to the test standards.

### 3.5. Thermo-mechanical characterization of the composites

A double cantilever bending mode DMA (TA Q-800 instrument) machine was used to measure the thermo-mechanical properties of the composites at an oscillation frequency of 1 Hz under a nitrogen atmosphere. The machine was run in a temperature range from 25 °C to 180 °C with a constant temperature ramp of 2 °C min<sup>-1</sup>. From these DMTA experiments, the storage modulus ( $E_o$ ) and loss factor ( $\tan \delta$ ) values of the tested specimens could be determined.

## 4. Results and discussion

### 4.1. Physical characterization of the fibres, preforms and composites

Fig. 3 shows SEM images of the surface topographies of jute fibres before and after alkali and sizing treatments. Untreated jute fibres were covered with cementitious materials (fat, waxes, hemicelluloses, and lignins) (see Fig. 3a). Alkali treatment removed most of this cementitious material, particularly hemicelluloses that are present in the interfibrillar network of the jute fibres.<sup>5</sup> After this treatment, very clean and rough jute fibre surfaces (see Fig. 3b) were obtained due to possible interactions between the hydroxyl groups of hemicelluloses and the sodium hydroxide functional group of the alkali solution. Aqueous sodium hydroxide ionized the hydroxyl groups of the jute fibres to form alkoxy groups, as shown in Fig. 5b. This is also in agreement with previous studies of jute fibres, where jute fibres were treated with low concentrations of alkali solution to remove impurities and thus change the surface regularity.<sup>1,8,9,25</sup> Thus, fibre uniformity was achieved using alkali treatment. In this work, PVA sizing material was applied to the fibres to bind individual fibres to each other. Fig. 3c shows an alkali-treated PVA-sized fibre surface, wherein the sizing

material can clearly be seen on the alkali-treated jute fibre. Tables 1 and 2 provide information about the physical properties of the jute and bamboo fibre preforms and their composites, respectively. It was observed that the thickness and area density of the dry fibre preforms changed upon the application of stitching and sizing treatments using untreated and alkali-treated jute fibre preforms. This might be related to changes in the fibre packing capacities of individual fibres in the preforms after the introduction of stitching, alkali, and sizing treatments.

In the case of the composites, alkali treatment and PVA sizing significantly improved the fibre volume fractions of the composites, as can be seen in Table 2. The densities of the composites greatly vary due to the effects of the treatments, as can also be seen in Table 2. In this work, the same dry fibre weight and jute fibre type were used for developing all the UD jute preforms and, subsequently, the jute and jute/fibre hybrid composites were subjected to the same compression pressure and curing time. Therefore, the observed changes in the fibre volume fractions of the developed composites are due to the sizing and alkali treatments and the stitching operations, which change the fibre packing capacities in jute fibres. We noticed a relatively lower fibre content in the cross-section of the UT composite, which is attributed to the presence of impurities and more technical fibres (single fibres cemented together) in the composites (see Fig. 3d). However, after alkali and sizing treatments, these impurities were easily removed and cementitious material in technical fibres also dissolved. As a result of this, the fibre content levels in all the treated composites significantly improved (the example of the BT composite is shown in Fig. 3e). SEM investigations were also carried out to see any defects present in the microscale cross-sections of the composites. No other porosity was observed except for luminal porosity in the developed composites in this work, and an example is shown here in Fig. 3f of the UT composite. Therefore, we did not consider the small percentages of voids present in the composites.

Table 2 The physical properties of the developed jute and jute/bamboo composites

Composite		Ply no.	Composite thickness (mm)	Volume fraction (%)			Composite density (g cm <sup>-3</sup> )
ID	Preform details			Jute	Bamboo	Total	
UT	Untreated fibres	8	2.66 ± 0.11	32	0	32 ± 2	1.19 ± 0.21
SUT	Stitched alkali-untreated fibres	8	2.78 ± 0.22	38	0	38 ± 3	1.20 ± 0.25
ST	Stitched alkali-treated fibres	8	2.80 ± 0.12	44	0	44 ± 2	1.24 ± 0.18
SUTB	Stitched alkali-untreated fibres with bamboo slices	9	2.84 ± 0.23	29	15	44 ± 3	1.22 ± 0.22
STB	Stitched alkali-treated fibres with bamboo slices	9	2.96 ± 0.21	29	18	47 ± 4	1.25 ± 0.24
BUT	Sized alkali-untreated fibres	8	2.68 ± 0.16	47	0	47 ± 1	1.23 ± 0.14
BT	Sized alkali-treated fibres	8	2.80 ± 0.25	48	0	48 ± 4	1.26 ± 0.14
BUTB	Sized alkali-untreated fibres with bamboo slices	9	2.94 ± 0.23	29	15	44 ± 2	1.22 ± 0.19
BTB	Sized alkali-treated fibres with bamboo slices	9	3.0 ± 0.22	26	19	45 ± 2	1.24 ± 0.11
BB	Bamboo slices	2	2.0 ± 0.19	0	66	66 ± 3	1.30 ± 0.22



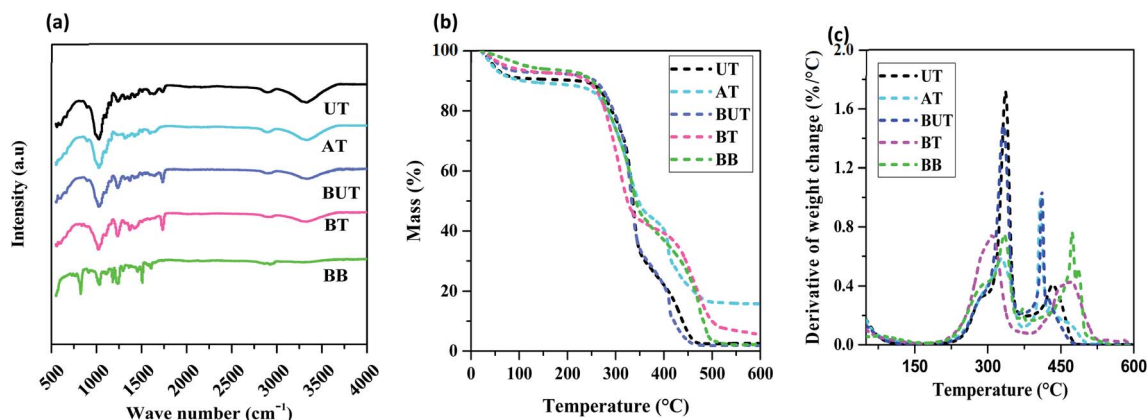


Fig. 4 (a) The FTIR spectra of different treated and untreated jute fibre samples. Thermogravimetric analysis: (b) mass loss vs. temperature and (c) the DTG curves of untreated and treated jute fibre samples.

#### 4.2. Chemical and thermal analysis

FTIR results for the chemical analysis of the treated fibres are shown in Fig. 4a. The characteristic bands of natural fibres are often related to the functional groups of cellulose and hemicelluloses. The presence of O–H groups (bending in-plane), C–O groups (stretching), and O–H groups (bending out-of-plane) is reflected in the spectral bands at  $1140\text{ cm}^{-1}$ ,  $1115\text{ cm}^{-1}$ , and  $980\text{ cm}^{-1}$ , respectively.<sup>26</sup> The bands in the range from  $1600\text{ cm}^{-1}$  to  $1420\text{ cm}^{-1}$  are attributed to the skeleton stretching vibrations of aromatic rings, which mainly arise from the presence of huge amounts of lignin and are clearly visible in the bamboo fibre (BB) and untreated fibre (UT) samples. Moreover, the strong peak intensity at  $1560\text{ cm}^{-1}$  indicated the presence of high amounts of carbonyl groups in the bamboo fibre (BB) sample.<sup>27</sup> These peak intensities were observed to reduce slightly after applying alkali treatment. The peak at  $1740\text{ cm}^{-1}$ , related to the acetyl and ester groups of hemicellulose and lignin, was visible in the cases of the untreated and treated sized (BUT and BT, respectively) jute fibres only. However, this peak was absent after the alkali treatment of jute fibres (AT). This observation confirmed the removal of hemicelluloses under the action of alkali treatment alone.<sup>5</sup> The peaks ranging from  $2700$  to  $2900\text{ cm}^{-1}$  indicate the C–H stretching vibrations of alkyl

groups in the aliphatic bonds of cellulose, lignin, and hemicelluloses.<sup>28</sup> Finally, the large peak at  $3200\text{ cm}^{-1}$  confirmed the presence of O–H stretching vibrations of hydroxyl groups in the cellulose molecules, which were more prominent in the case of UT jute fibres. However, this peak intensity was reduced after the introduction of alkali treatment, with or without sizing. Therefore, the FTIR data indicated the retention of many of the functional groups present in the untreated jute and bamboo fibres, with additional functional groups present after sizing treatment and the removal of hemicelluloses upon alkali treatment.

The thermal stabilities of untreated and treated jute fibres were analysed using a TGA analyser. TGA graphs are shown in Fig. 4b. The onset temperature of the AT fibres was reduced, probably due to the removal of carbon material (waxes, pectin, lignin, and hemicelluloses) from the fibre surfaces.<sup>29,30</sup> The thermal stabilities of untreated jute fibres (UT) and bamboo fibres (BB) were found to be similar in terms of their onset and final points, corresponding weight loss percentages, and residue percentages. For BUT (sized alkali-untreated) fibres, the thermal stability was observed to increase from  $266\text{ °C}$  to  $279\text{ °C}$ , almost  $13\text{ °C}$  higher than the UT fibres. This was possibly due to hydroxyl groups present in the PVA sizing material and hydroxyl groups in the untreated jute fibres,

Table 3 The tensile and flexural properties of the developed UD jute fibre composites

Fibre type	Composite ID	Tensile strength (MPa)	Flexural strength (MPa)	Tensile modulus (GPa)	Flexural modulus (GPa)	Tensile strain (%)	Flexural strain (%)
Untreated	UT	$122 \pm 15$	$52 \pm 9$	$10 \pm 1$	$6.5 \pm 1$	$1.7 \pm 0.25$	$15 \pm 1$
	SUT	$117 \pm 5$	$129 \pm 6$	$10 \pm 0.5$	$6.4 \pm 1$	$1.43 \pm 0.2$	$9 \pm 2$
Stitched	ST	$144 \pm 10$	$157 \pm 10$	$11 \pm 1$	$7 \pm 1$	$1.56 \pm 0.25$	$14 \pm 2$
	SUTB	$172 \pm 30$	$261 \pm 25$	$11 \pm 1$	$10 \pm 0.5$	$1.58 \pm 0.3$	$10 \pm 2$
	STB	$131 \pm 10$	$307 \pm 13$	$7 \pm 0.5$	$9 \pm 0.5$	$1.98 \pm 0.5$	$7 \pm 1.5$
	BUT	$110 \pm 3$	$170 \pm 9$	$13 \pm 1$	$8.5 \pm 1$	$1.07 \pm 0.1$	$13 \pm 1$
Sized	BT	$176 \pm 18$	$194 \pm 8$	$16 \pm 2$	$8 \pm 1$	$1.5 \pm 0.32$	$12 \pm 2$
	BUTB	$130 \pm 17$	$160 \pm 30$	$8 \pm 1$	$10 \pm 1$	$1.64 \pm 0.2$	$11 \pm 2$
	BTB	$101 \pm 18$	$195 \pm 16$	$6 \pm 0.5$	$6.5 \pm 0.6$	$1.65 \pm 0.3$	$10 \pm 1$
Bamboo	BB	$203 \pm 45$	$44 \pm 6$	$9 \pm 1$	$8 \pm 2$	$2.55 \pm 0.28$	$6.0 \pm 1$



including polysaccharides (hemicelluloses, pectin, lignin), reacting together to form hydrogen bonds, thus delaying the onset degradation temperature. However, the weight loss was found to be significantly higher in the case of the BUT jute fibres. An increase in char residue was noticed only for AT (alkali-treated) fibres (see Fig. 4b). The increased amount of char could be related to the stabilization of otherwise high rates of free-radical formation in the lignin–cellulose complexes created during the alkali treatment of fibres.<sup>31</sup> DTG curves were also plotted in Fig. 4c, where three peaks were observed for treated/untreated fibres: the first one indicates moisture release; the second one is related to the degradation of hemicelluloses; and the third one indicates the degradation of the non-cellulosic parts of the cellulose fibres.<sup>32</sup> The first degradation shoulder peak was located at around 290 °C for UT fibres. This was also visible for the BUT and BB fibres. More particularly, this peak arises from the thermal decomposition of hemicelluloses present in those fibres.<sup>23</sup> After alkali treatment, this peak was not seen in the case of AT fibres, and this was also true in the case of BT fibres, which applied PVA sizing treatment to alkali-treated jute fibres. Similar observations were reported in previous studies<sup>8,26</sup> of jute, hemp, and coir fibres. This clearly indicates that the alkali- and sizing-treatment of jute fibres have great influence on the thermal properties.

### 4.3. Tensile properties of the composites

The tensile properties of stitching- and sizing-based UD preform jute and jute/bamboo hybrid composites were tested and compared in this work; details are provided in Table 3. Jute fibres contain significant amounts of non-cellulosic materials (pectin, lignin, hemicelluloses, and waxes), which can result in poor mechanical performance being shown by composites. As a result of this, the untreated jute fibre composite (UT) here showed a low tensile modulus of 10 GPa and a tensile strength

of only 122 MPa. In terms of the stitched-preform-based composites, the stitched alkali-untreated composite (SUT) unexpectedly showed no changes in tensile properties, despite a slight increase in the fibre volume fraction. It is known that the mechanical properties of fibre-reinforced composites mainly depend on the tensile properties of the reinforcer, the volume fraction, and the strength and toughness of the matrix.<sup>33,34</sup> These observed unchanged tensile properties of the SUT composite might be related to fibre damage during the stitching operations, caused by the mechanical action of sewing needles (see Table 3). It was also observed in a previous study that sewing operations on natural fibres can damage the structural integrity of jute fibres, which may result in poor mechanical properties.<sup>13</sup> It was observed that the stitched alkali-treated composite (ST) showed a slight improvement in tensile properties, with tensile modulus and strength values of 11 GPa and 144 MPa, respectively. These improvements are attributed to an improvement in the interfacial properties between the stitched alkali-treated jute fibres and the epoxy matrix due to chemical interactions between the relatively greater number of hydroxyl groups in the alkali-treated jute fibres (compared to the untreated jute fibres) and the oxygen functional groups of the epoxy network.<sup>35</sup> Possible interactions between jute fibre cellulose, sodium hydroxide, and epoxy resin are given in Fig. 5b and c.

In order to achieve further improvements in the mechanical properties of the stitched UD jute fibre composites, a bamboo slice was placed in between the 8 layers of the stitching-based preform, creating both alkali-treated (STB) and untreated (SUTB) stitched UD jute fibre composites. No changes were observed in the tensile modulus values of the composites, whereas a significant improvement was achieved in the tensile strength of the SUTB composite, which showed a value of 172 MPa, an almost 41% improvement in tensile strength

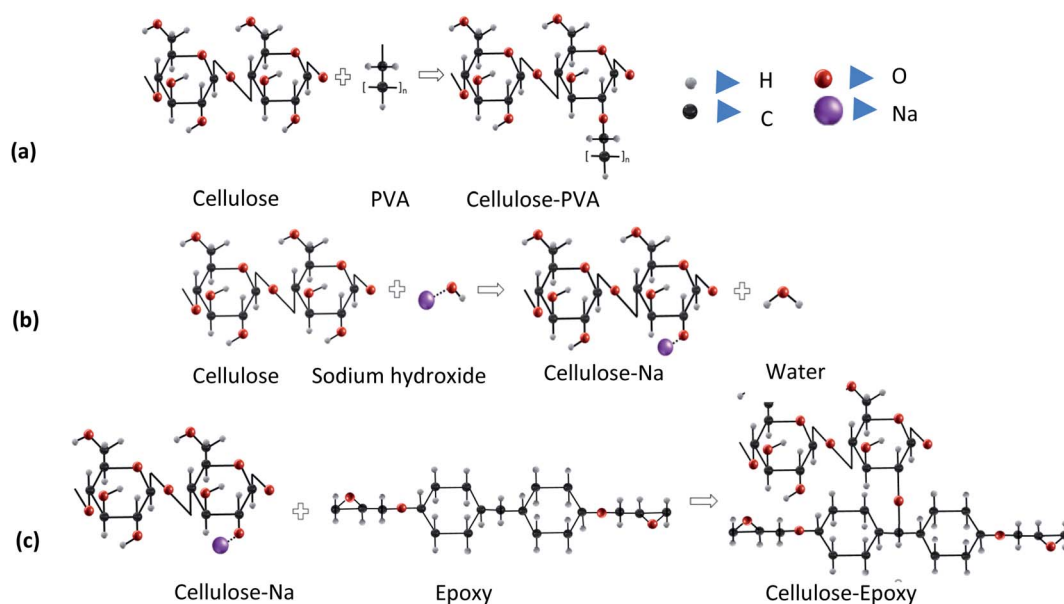


Fig. 5 Possible chemical interactions between the cellulose molecular structures of jute fibres and (a) polyvinyl alcohol (PVA), (b) sodium hydroxide, and (c) epoxy.



compared to the UT composite (see Table 3). However, the tensile properties were found to be reduced in the case of the STB composite. These significant changes in tensile properties are linked to several reasons. For example, bamboo slices have a high tensile strength (203 MPa) when they are reinforced with an epoxy matrix (BB composite). In this regard, based on the rule of mixtures, the mechanical properties of the reinforcement directly influence the improvement in the tensile strength of the SUTB composite. Also, the parallel arrangement of the fibrils of the bamboo slices allows the composites to bear a higher applied load. The reduction in the tensile properties of the STB composite could be related to the incompatibility of alkali-treated jute fibres and alkali-untreated bamboo slices, resulting in a poor interfacial network between the fibres and the matrix, which could be responsible for the early failure of the STB composite.

PVA-sizing-based UD preforms were also developed and used to manufacture UD jute composites that were tested in this work. The tensile modulus of the sized alkali-untreated preform composite (BUT) was seen to increase to 13.5 GPa, although no improvement was found in the tensile strength value. The tensile modulus was improved by almost 35% compared with the UT composite. This could be due to strong fibre-to-fibre connections created by reactions between the -OH groups of the PVA sizing material and the jute fibres, together with a higher degree of fibre alignment (see Fig. 5a). The PVA-sized alkali-treated (BT) composite showed maximum increases in the modulus (by 62%) and strength (by 44%) compared with the UT composite. The corresponding values of the tensile modulus and strength were measured to be 16 GPa and 176 MPa, respectively. This significant improvement was achieved because of several possible reasons. Firstly, there were synergistic effects due to the PVA-sizing and alkali treatments on the jute fibres and their interactions with the epoxy matrix. The greater numbers of hydroxyl groups on the PVA-sized jute fibre surfaces increased the wettability of the jute fibres, and when these sized jute fibres were reinforced with epoxy matrix, strong hydrogen bonds were formed together with amino-peptide bonds involving the amine hardener in the matrix.<sup>5</sup> Secondly, increased amounts of fibrillation and fibre uniformity occurred due to the action of the alkali treatment, thus increasing the load-bearing capacity of the fibres upon tensile loading. Thirdly, the PVA-sizing of alkali-treated fibres promotes strong adherence between adjacent single fibres, thereby increasing the fibre content in the composites upon compression. As discussed earlier, jute fibres are very susceptible to alkali treatment, which performs two actions (cleaning and separating elementary fibres from technical fibres). This combination of alkali and sizing actions resulted in the enhancement of the fibre volume fraction in the BT composite during the composite manufacturing process in this work, as the same compaction and curing processes were used for all composites developed herein. Therefore, here, these two treatments (alkali and sizing), leading to higher fibre content levels, played a vital role in increasing the tensile properties of the BT composite, as we know from the rule of mixtures that with an increase in the fibre content, the mechanical properties can proportionally increase

in a composite. However, a decrease in tensile properties was observed for the alkali-treated PVA-sized UD jute composite with interleaved bamboo slices (BTB), similar to the STB composite, because of incompatibility between the alkali-treated jute fibres and bamboo slices.

#### 4.4. Flexural properties of the composites

The flexural properties (flexural modulus and flexural strength) of the developed UD jute fibre and jute/bamboo hybrid composites were tested and analysed, and the results are depicted in Table 3. All the values in the table are average values from five specimens for each sample type, with the standard deviation values also given. In this study, the flexural modulus and strength values for the UT composite were measured to be 6.5 GPa and 52 MPa, respectively. It was observed that all stitched (SUT, ST, SUTB, and STB) and sized (BUT, BT, BUTB, and BTB) preform based composites showed significant improvements in flexural properties compared with the UT composite (see Table 3). The UT composite showed the lowest flexural properties, which was possibly due to the presence of impurities (pectin, waxes, hemicelluloses, lignin, jute batch oil, *etc.*), resulting in poor interfacial adhesion between the fibres and the matrix and, therefore, the composite showed a poor bending-load-bearing capacity. Related to this, stress concentration occurs at the interfaces of composites, leading to crack development and overall deformation in composites upon bending.<sup>36,37</sup> For the SUT composite, the flexural strength was improved by 147% compared with the UT composite due to the stitching of the fibres. A further increase was visible for the ST composite, which was related to both the alkali and stitching treatment of the fibres. The sized-preform-based BUT composite exhibited a flexural modulus of 8.66 GPa and flexural strength of 169.37 MPa. A similar trend was observed for the BT composite as for the ST composite, with the use of both alkali and sizing treatments improving the flexural strength to 194.26 MPa, which was almost 14% higher than the sized alkali-untreated composite (BUT) (see Table 3). The increase in the flexural properties of the ST and BT composites is attributed to the alkali treatment as well as the stitching and sizing operations on the preforms, which created higher regularity along the fibre length and also better fibre packing in the composites, thus enhancing the bending-load-bearing capacity compared to the untreated composite (UT).<sup>2,38</sup> Using bamboo slices in the stitching-based composites, the maximum flexural modulus (10 GPa) was measured for the SUTB composite, whereas the maximum flexural strength (307 MPa) was achieved for the STB composite. This improvement was due to the addition of an extra layer of naturally highly aligned bamboo slice and its interactions with the stitched preform, which ultimately provided extra support allowing higher bending-load resistance to be shown by the composites. However, no trend or positive effect was observed when bamboo slices were incorporated with sized-preform-based (BUTB and BTB) composites. This could be due to the incompatibility of the sized jute fibres with the bamboo slices, creating poor interfacial properties, which did not allow for higher stress tolerance upon exposure to bending



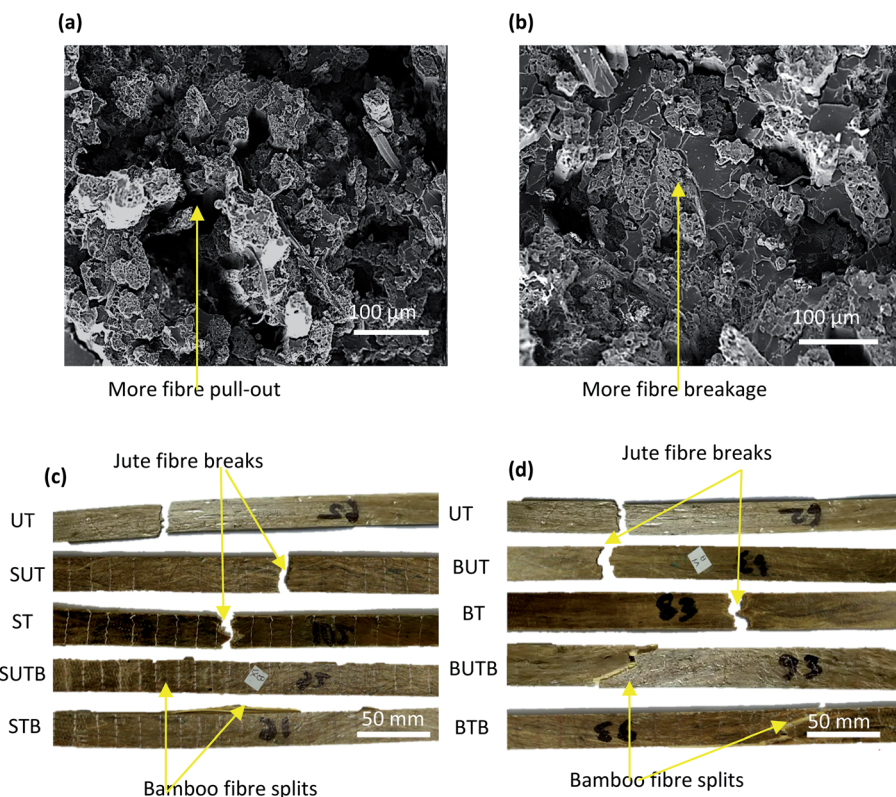


Fig. 6 SEM images of the fracture surfaces of (a) untreated (UT) and (b) stitched alkali-treated (ST) composites. Digital images of specimens after tensile testing: (c) stitched-preform-based and (d) sized-preform-based jute fibre composites.

loads. Due to the significant contribution of the bamboo slices to the improvements of the flexural properties of the stitching-based preform composites (SUTB and STB), further detail studies are necessary to elucidate the exact mechanics of bamboo reinforcement.

#### 4.5. Fractographic analysis

Broken specimens obtained after tensile and flexural testing were examined using SEM and digital imaging to see the

fracture topographies of the composites, as shown in Fig. 6. For the UT composite, failure occurred predominantly as a result of a combination of extreme fibre pull-out and weak interfacial bonding. Fibres came out from the matrix unevenly in the broken specimen, as seen in Fig. 6a. In contrast, the ST composite showed even fibre breakage (see Fig. 6b), which indicates an improvement in the fibre packing and interfacial bonding between the fibres and epoxy matrix. The same observations were also found in the sizing-based preform

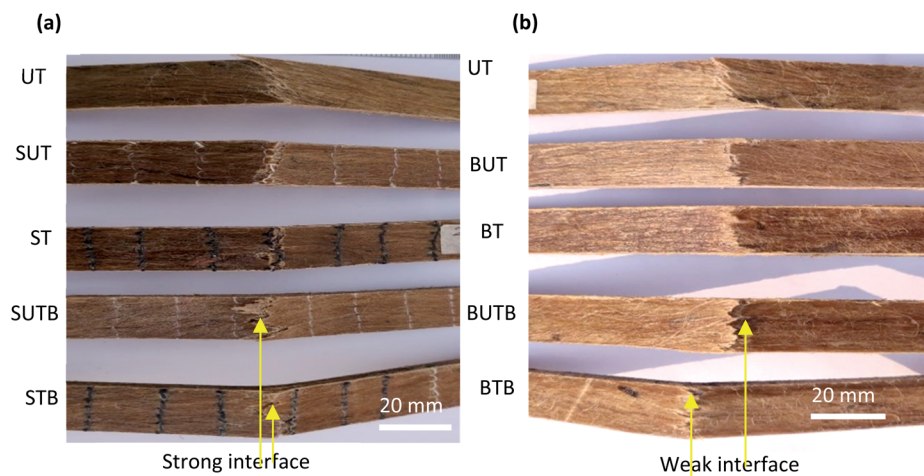


Fig. 7 (a) A digital image of stitched specimens after flexural testing. (b) A digital image of sizing-based specimens after flexural testing.



composites, which are not shown here. Fig. 6c and d show the fracture surfaces of stitched and sized preform based jute composite specimens after tensile tests, respectively. Both the stitched and sized preform based composites showed clear and linear fibre breakages at the fracture surfaces, except the bamboo/jute composites, wherein no linear fibre breakages were observed as fibres were split rather than clearly broken, as can be seen in Fig. 6c and d. These observations are also similar to those found in a study of UD jute fibre composites based on raw hackled jute slivers reported in the literature.<sup>1</sup> Fig. 7 shows both stitched and sized UD composite specimens after flexural testing. Only the stitched-preform-based composites with bamboo slices (SUTB, STB) demonstrated strong bending support, reflected in the buckling of the tested specimens, whereas the sizing-based bamboo/jute composites (BUTB and BTB) showed larger splits in the fibres after flexural testing.

In order to develop further understanding of the dynamic mechanical behaviors of the stitched- and sized-preform-based jute composites over a wide temperature range, DMTA analysis was carried out. For this, only the SUTB and BT composites were studied and compared against the UT composite. From the above-discussed tensile and flexural properties, it was found that the SUTB and BT composites demonstrated balanced improvements both in tensile and flexural properties out of all the stitched- and sized-preform-based composites and, because of this, they were studied further *via* DMTA analysis.

#### 4.6. Dynamic mechanical thermal analysis (DMTA)

Fig. 8a illustrates the variations in the storage modulus ( $E'$ ) values of the UT, SUTB, and BT composites as a function of temperature at a frequency of 1 Hz. The DMTA results provide important information regarding the stiffness, degree of crosslinking, and fibre-matrix interfacial bonding in the composites. Here, all composite samples showed the pattern of the  $E'$  value decreasing with an increase of temperature, as the polymer chains became flexible at higher temperatures; then there was a sharp decline in the  $E'$  value in the glass transition

region due to the molecular mobility of the polymer chains above the glass transition temperature ( $T_g$ ). The BT and SUTB composites showed notable increases in the  $E'$  values compared to the UT composite. Considering the BT and SUTB composite samples, the BT sample exhibited the highest  $E'$  value, which also agrees with the higher tensile properties of the BT composite noticed in this work. This increase could be linked to improved fibre-matrix interfacial adhesion brought about through the PVA-sizing and alkali treatment, enabling the BT composite to carry and transfer stress at the interface.

The mechanical damping factor, or  $\tan \delta$ , is presented in Fig. 8b.  $\tan \delta$  is the ratio of the loss modulus ( $E''$ ) to the storage modulus ( $E'$ ), and it provides information about the material damping behaviour related to the impact properties, energy absorption/dissipation mechanism, glass transition temperature, *etc.* The  $\tan \delta$  value was seen to increase with temperature, reaching a maximum in the glass transition region and then decreasing above the glass transition region (the rubbery region). This was observed for the UT, SUTB, and BT composites. The BT composite sample showed a slight shift in the  $\tan \delta$  peak position towards a higher temperature compared to the UT and SUTB composites. This indicates a small rise in the  $T_g$  value, which is related to the lower molecular mobility of the polymer chains and is also in agreement with the better stiffness observed through the higher storage modulus values of the BT composite. An additional small hump was observed for the BT composite above the glass transition temperature in the  $\tan \delta$  curve because of either the movement of dry jute fibre cellulose towards  $T_g$  (ref. 39) or the existence of an entrapped resin region with a different network structure close to the interface, causing higher temperature thermal relaxation.<sup>40</sup> The UT composites showed a higher  $\tan \delta$  curve peak than the SUTB and BT composites, as expected, due to poor fibre-matrix adhesion increasing the polymer chain mobility and damping factor of the composite. The BT composite displayed slightly higher  $\tan \delta$  values than SUTB, which might be due to the combined effects of the PVA and alkali treatment leading to an increase in both damping and adhesion at the fibre-matrix interface.

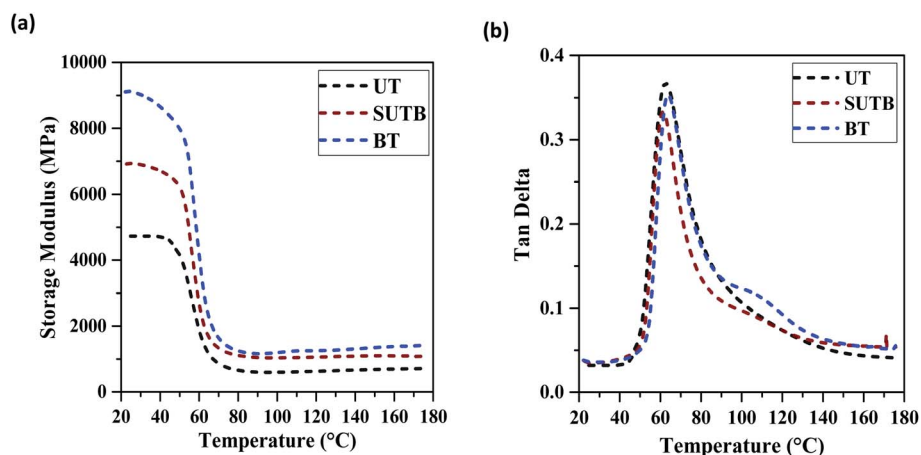


Fig. 8 The dynamic mechanical thermal analysis of jute fibre composites: (a) storage modulus versus temperature and (b) tan delta versus temperature curves.



## 5. Conclusions

Unidirectional (UD) jute fibre preforms were manufactured using novel stitching and PVA-sizing techniques for the first time in this work to achieve jute composites with higher mechanical performance. Alkali-treated and untreated fibres were used in both techniques. Bamboo slices were also added in the middle of both stitched and sized preforms during the manufacturing of the composites to see the effects of using bamboo slices on the mechanical performances of the jute/bamboo hybrid composites. From the results obtained, the key points can be concluded as follows:

- SEM images showed that alkali and PVA-sizing treatments affect the fibre surfaces, since clean and rough fibre surfaces were found upon the removal of fibre impurities *via* alkali treatment, while fibre bonding was clearly seen after PVA-sizing treatment. These observations were further confirmed *via* FTIR studies.

- Only PVA-sizing treatment was capable of increasing the thermal stability of the fibres in TGA investigations due to the enhanced interactions between the –OH groups of PVA and jute fibres.

- Tensile and flexural property analysis clearly indicated that both UD stitched and PVA-sized preforms can be successfully used to significantly improve the mechanical performances of jute composites; the PVA-sized alkali-treated (BT) composite showed the most promising results for use in load-bearing applications. This was observed to occur because of better interconnection between PVA-sizing and alkali-treated fibres, causing more fibre fibrillations and a stronger fibre-matrix interface, leading to the composite showing a higher load-carrying capacity.

- Bamboo slices can be added to jute composites to further improve their mechanical performance only when it comes to the stitched alkali-untreated jute preform based composite (SUTB); it displayed a significant positive increase in mechanical properties due to the highly aligned bamboo fibres undergoing strong interactions with the stitched jute fibres.

- The bamboo slices resulted in no improvement in the mechanical properties of the PVA-sized and stitched alkali-treated UD jute fibre preforms because of incompatibility and poor interfacial properties of the bamboo slices with sizing- and alkali-treated jute fibre preforms.

The newly developed jute fibre UD preforms will be investigated further in future work, examining areas such as the effects of the linear density of jute fibres on the mechanical performances of UD preforms, *etc.*, in order to scale up manufacturing processes to make preforms with larger dimensions that can be brought to market commercially. The significant improvements in the mechanical properties of the newly developed novel UD architecture jute composites achieved in this work will be helpful for promoting the use of cost-effective jute fibre bio-composites for lightweight structural composite applications.

## Author contributions

M. Hasan – manufacturing composites, mechanical testing, analysis of data, and image processing; A. Saifullah –

investigation, writing-original draft, evaluation of the chemical, thermal, and thermo-mechanical properties, and analysis; H. Dhakal – investigation, overall review, and supervision of the work. S. Khandaker – investigation of experimental work, and data analysis. F. Sarker – main conceptualization and design of the experimental work, writing-original draft, review, editing, and supervision.

## Conflicts of interest

There are no conflicts to declare.

## Acknowledgements

The authors are grateful to UMC Jute Mill authority for supplying the jute fibres used in this project.

## References

- 1 F. Sarker, P. Potluri, S. Afroj, V. Koncherry, K. S. Novoselov and N. Karim, *ACS Appl. Mater. Interfaces*, 2019, **11**, 21166–21176.
- 2 J. Gassan and A. K. Bledzki, *Compos. Sci. Technol.*, 1999, **59**, 1303–1309.
- 3 F. Sarker, M. Akonda and D. U. Shah, *Materials*, 2020, **13**, 1–16.
- 4 S. Goutianos, T. Peijs, B. Nystrom and M. Skrifvars, *Appl. Compos. Mater.*, 2006, **13**, 199–215.
- 5 F. Sarker, N. Karim, S. Afroj, V. Koncherry, K. S. Novoselov and P. Potluri, *ACS Appl. Mater. Interfaces*, 2018, **10**, 34502–34512.
- 6 M. T. Zafar, S. N. Maiti and A. K. Ghosh, *RSC Adv.*, 2016, **6**, 73373–73382.
- 7 A. K. Bledzki and J. Gassan, *Prog. Polym. Sci.*, 1999, **24**, 221–274.
- 8 A. Roy, S. Chakraborty, S. P. Kundu, R. K. Basak, S. Basu Majumder and B. Adhikari, *Bioresour. Technol.*, 2012, **107**, 222–228.
- 9 M. Ashadujjaman, A. Saifullah, D. U. Shah, M. Zhang, M. Akonda, N. Karim and F. Sarker, *Mater. Res. Express*, 2021, **8**, 055503.
- 10 A. Mukherjee, P. K. Ganguly and D. Sur, *J. Text. Inst.*, 2008, **84**, 348–353.
- 11 N. Karim, F. Sarker, S. Afroj, M. Zhang, P. Potluri and K. S. Novoselov, *Adv. Sustainable Syst.*, 2021, **5**, 2000228.
- 12 M. Z. Rong, M. Q. Zhang, Y. Liu, Z. W. Zhang, G. C. Yang and H. M. Zeng, *J. Compos. Mater.*, 2002, **36**, 1505–1526.
- 13 M. Ravandi, W. S. Teo, L. Q. N. Tran, M. S. Yong and T. E. Tay, *Composites, Part B*, 2017, **117**, 89–100.
- 14 F. A. Almansour, H. N. Dhakal and Z. Y. Zhang, *Compos. Sci. Technol.*, 2018, **154**, 117–127.
- 15 A. Saifullah, B. Thomas, R. Cripps, K. Tabeshfar, L. Wang and C. Muryn, *Polym. Eng. Sci.*, 2018, **58**, 63–73.
- 16 V. Fiore, T. Scalici, D. Badagliacco, D. Enea, G. Alaimo and A. Valenza, *Compos. Struct.*, 2017, **160**, 1319–1328.
- 17 Z. Al-Hajaj, R. Zdero and H. Bougherara, *Composites, Part A*, 2018, **115**, 46–56.



- 18 S. Khandai, R. K. Nayak, A. Kumar, D. Das and R. Kumar, *Mater. Today: Proc.*, 2019, **18**, 3835–3841.
- 19 R. Kumar, K. Singh, E. Gogna, H. R. Sinha and A. K. Sahoo, *Int. J. Integr. Eng.*, 2020, **12**, 104–115.
- 20 Y. Yu, X. Huang and W. Yu, *Composites, Part B*, 2014, **56**, 48–53.
- 21 J. W. Holmes, P. Brøndsted, B. F. Sørensen, Z. Jiang, Z. Sun and X. Chen, *Wind Eng.*, 2009, **33**, 197–210.
- 22 A. Orue, A. Jauregi, U. Unsuain, J. Labidi, A. Eceiza and A. Arbelaiz, *Composites, Part A*, 2016, **84**, 186–195.
- 23 H. N. Dhakal, Z. Y. Zhang, R. Guthrie, J. Macmullen and N. Bennett, *Carbohydr. Polym.*, 2013, **96**, 1–8.
- 24 J. Flynn, A. Amiri and C. Ulven, *Mater. Des.*, 2016, **102**, 21–29.
- 25 K. Singh, D. Das, R. K. Nayak, S. Khandai, R. Kumar and B. C. Routara, *Mater. Today: Proc.*, 2019, **26**, 2094–2098.
- 26 V. Fiore, T. Scalici, F. Nicoletti, G. Vitale, M. Prestipino and A. Valenza, *Composites, Part B*, 2016, **85**, 150–160.
- 27 B. M. Pejic, M. M. Kostic, P. D. Skundric and J. Z. Praskalo, *Bioresour. Technol.*, 2008, **99**, 7152–7159.
- 28 A. Orue, A. Jauregi, C. Peña-Rodriguez, J. Labidi, A. Eceiza and A. Arbelaiz, *Composites, Part B*, 2015, **73**, 132–138.
- 29 A. R. Horrocks and D. Price, *Advances in fire retardant materials*, 2008.
- 30 K. L. Pickering, G. W. Beckermann, S. N. Alam and N. J. Foreman, *Composites, Part A*, 2007, **38**, 461–468.
- 31 B. Kandola, F. Sarker, P. Luangtriratana and P. Myler, *Coatings*, 2016, **6**, 22.
- 32 J. Müssig and K. Haag, *Biofiber Reinforcements in Composite Materials*, Elsevier, 2015.
- 33 Z. Mahboob, I. El Sawi, R. Zdero, Z. Fawaz and H. Bougherara, *Composites, Part A*, 2017, **92**, 118–133.
- 34 Z. Mahboob and H. Bougherara, *Composites, Part A*, 2018, **109**, 440–462.
- 35 E. Pisanova and E. Máder, *J. Adhes. Sci. Technol.*, 2000, **14**, 415–436.
- 36 T. H. Nam, S. Ogihara, N. H. Tung and S. Kobayashi, *Composites, Part B*, 2011, **42**, 1648–1656.
- 37 E. Gogna, R. Kumar, A. K. Sahoo and A. Panda, in *Lecture Notes in Mechanical Engineering*, 2019, pp. 459–467.
- 38 A. Chatterjee, S. Kumar and H. Singh, *Compos. Commun.*, 2020, **22**, 100483.
- 39 A. K. Rana, B. C. Mitra and A. N. Banerjee, *J. Appl. Polym. Sci.*, 1999, **71**, 531–539.
- 40 K. N. E. Verghese, R. E. Jensen, J. J. Lesko and T. C. Ward, *Polymer*, 2001, **42**, 1633–1645.

